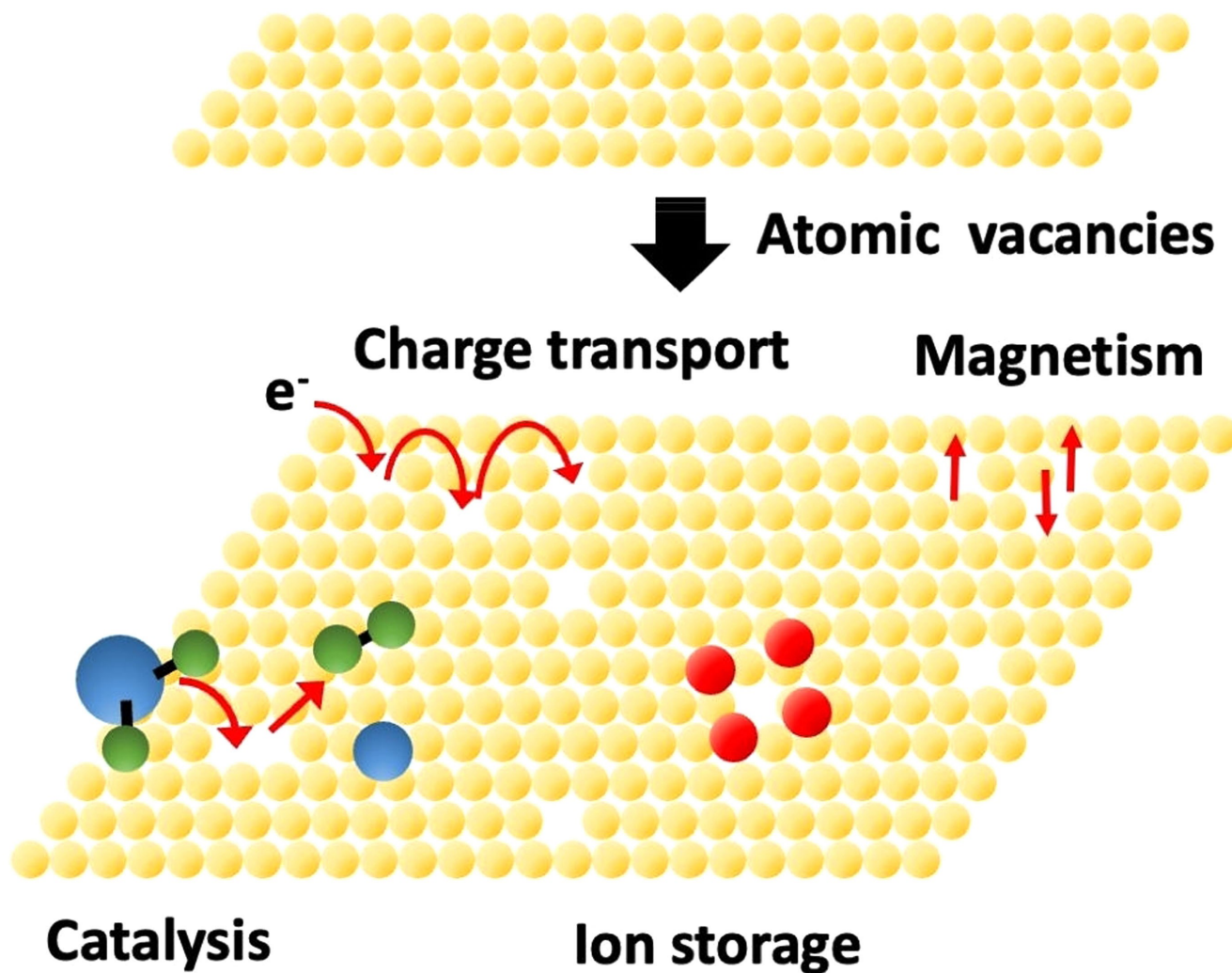


Atomic Vacancies in Transition Metal Dichalcogenides: Properties, Fabrication, and Limits

Massimiliano Cavallini* and Denis Gentili^[a]



Structural defects, such as heteroatoms or atomic vacancies, are always present in materials and significantly affect their physical properties, in both positive or unwanted ways. Interestingly, defects generate an impressive range of functionalities in many materials, such as catalysis, electrical and thermal conductivity tuning, thermoelectricity, enhanced ion storage, magnetism, and others. These properties enable the use of defective

materials in a great variety of technological applications. Here we review the principal properties generated by atomic vacancies in 2D compounds and thin films of transition metal dichalcogenides and the most consolidated methods for their formation and engineering. Eventually, we critically analysed the most important advantages, the limits and the current open challenges.

1. Introduction

Defects are always present in all manufactured materials and significantly affect their chemical and physical properties. Interestingly, although defects have a detrimental effect on some properties, such as a decrease in mechanical stability and the dramatic change of the charge transport properties, they can also generate an impressive number of functionalities, such as catalysis, tuning of electrical and thermal conductivity, thermoelectricity, ion storage, enhance the sensing capabilities magnetism and other. These functionalities make defective materials suitable for a variety of technological applications (Figure 1).^[1] The most striking example of the impact of defects on science and technology is the doping of silicon which, over the past 70 years or so, has allowed the extraordinary development of micro- and nano-electronics. Practically, the doping of semiconductors consists of introducing defects in the material, usually through the introduction of a heteroatom which introduces a localized electronic state in the semiconductor bandgap (midgap states).

Defects define material properties, and defect engineering optimizes a defective material for specific applications. Almost all papers on the study of defects invoke defect engineering as the way to devise materials for technological applications. Many excellent review articles are dedicated to defect engineering,^[1] some of them devoted to atomic vacancies^[2] and the role of defect distribution.^[3] However, due to the extent of the topic and its impressive rate of development, more specific review articles with different points of view and innovative types are needed to inspire future research, to evaluate the state of the art, problems and perspectives of such a stimulating topic.

Here we review atomic vacancies in low dimensional systems (i.e., 2D compounds and films made of a few monolayers) of transition metal dichalcogenides (TMD) as they are the most studied system, as proved by the impressive number of papers published weekly. In this article, we first briefly describe, in general, the different types of atomic vacancies in TMDs (Sect. 2), followed by a general overview of the principal properties generated by atomic vacancies (Sect. 3).

Section 4 discusses the principal method developed for defect formation and engineering and how they can be advantageously exploited in various fields. The review concludes (Sect. 5) with a summary of the most important results obtained so far, together with a discussion on the open problems and future challenges for the engineering of defective materials. We aim to increase awareness in the chemistry and material science communities that an unwanted phenomenon, such as the formation of atomic vacancies, can be an extraordinary opportunity to impart unprecedented functionalities to materials, enhancing their efficiency and versatility in practical applications.

2. Atomic Vacancies

The most common atomic vacancies are single atom vacancies (V_A) formed by removing a single metallic or non-metallic atom from the crystal lattice of a material. Multi-atomic vacancies, formed by removing more than one atom, are often present in many materials but are not as common as V_A . Multi-atomic vacancies are also more complex and more challenging to control, and often their detrimental effects are higher than the beneficial one.^[4] Figure 2 shows some examples directly observed by STEM atomic-resolution images of four different types of atomic and multi-atom vacancies commonly observed in MoS_2 : monosulfur vacancy (V_S), disulfur vacancy (V_{S_2}), vacancy complex of Mo near three sulfur atoms (V_{MoS_3}), and vacancy complex of Mo near three disulfur pairs.^[5]

Atomic vacancies, for example, in semiconductors, act as dopants generating midgap states which alter the spatial homogeneity of electronic states generating the functionalities of the material.^[6] Midgap states are generated by the reorganization of electron density around the vacancy. For example, in



Figure 1. Most significant properties and functionalities generated by atomic vacancies in transition metal dichalcogenides.

[a] Dr. M. Cavallini, Dr. D. Gentili
Istituto per lo Studio dei Materiali Nanostrutturati, (ISMN)
Consiglio Nazionale delle Ricerche (CNR)
Via P.Gobetti 101, Bologna (Italy)
E-mail: massimiliano.cavallini@cnr.it

© 2022 The Authors. ChemPlusChem published by Wiley-VCH GmbH. This is an open access article under the terms of the Creative Commons Attribution Non-Commercial License, which permits use, distribution and reproduction in any medium, provided the original work is properly cited and is not used for commercial purposes.

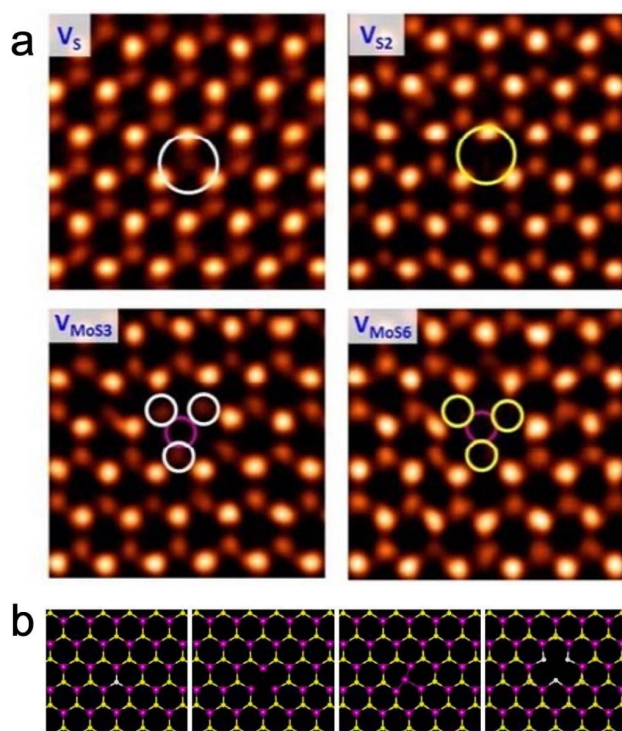


Figure 2. Most common atomic vacancy defects in MoS₂. (a) Atomic resolution ADF images of V_S, V_{S2}, MoS₂ and V_{MoS3}. (b) Related structural models of atomic vacancies observed shown in (a). From left to right: V_S, V_{S2}, MoS₂ and V_{MoS3}. Purple, yellow, and white balls represent Mo, top layer S, and bottom layer S, respectively. Figure adapted with permission from ref. 5. Copyright 2013 American Chemical Society.

defective MoS₂, sulphur vacancies (V_S), the most energetically stable defects^[1b] cause electron distribution changes in the surrounding Mo atoms (mainly within a 5 Å radius surrounding the V_S) generating the localized midgap states below the conduction band minimum.^[6] Importantly, generally speaking, the presence of limited density, the atomic vacancies has no significant effects on the long-range crystalline structure of the materials.^[7]

Midgap states generated by the defects induce a significant modulation of the band gap which gives rise to, or enhances, a variety of functional properties. Figure 3 shows the evolution of the band structure of two representative materials, such as WS₂

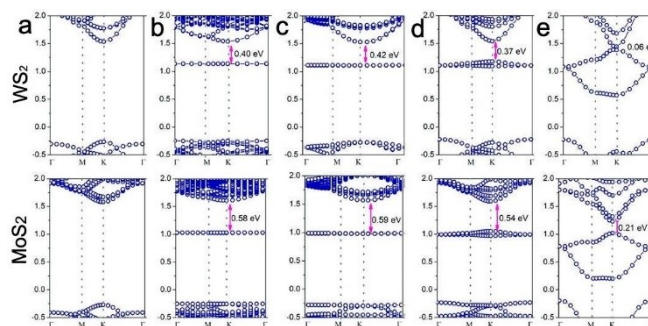


Figure 3. Band structure evolution of WS₂ (top) and WS₂ (bottom) on varying V_S densities: a) 0%, b) 1.6%, c) 2.8%, d) 6.3%, and e) 25.0% and the changes of midgap states with respect to the conduction band of the compounds. Figure adapted from ref. 6a with permission. Copyright 2013 Wiley-VCH GmbH, Weinheim.

and MoS₂, on varying the density of sulphur atomic vacancies from 0% to 25%.^[6a]

3. Properties Generated by Atomic Vacancies

Atomic vacancies generate an impressive number of new functionalities, some of the most important are summarized in Figure 1.

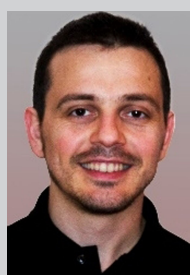
3.1. Optical

The modulation of the band gap gives rise to non-linear optical processes such as second harmonic generation,^[8] and more peculiar phenomena such as the formation of negative trions,^[9] a quasi-particle composed of two electrons and a hole which has no analogue in conventional semiconductors. Changes in optical properties are often detected by photoluminescence.^[10] Defects induce peak shifts of several tens of nanometres, proportional to the percentage of the defect density, and lead to new features in the spectra with significant changes in exciton life-times.^[11]

Moreover, the Raman spectra change dramatically due to the modification of phonon modes.^[11] Figure 4 shows an example of the effects on photoluminescence and Raman



Massimiliano Cavallini is Director of research at CNR-ISMN where he heads the multidisciplinary group of "Nanotechnology of Multifunctional Materials". He received a Laurea cum Laude in 1995 and PhD in Chemistry in 1999 from the University of Florence. His multidisciplinary research spans from nanofabrication, nanopatterning, nano-electrochemistry for nanofabrication, technological applications of unwanted phenomena such as dewetting and polymorphism, information storage and development of time-temperature integrators devices.



Denis Gentili is a research scientist at the ISMN-CNR. He graduated summa cum laude in Industrial Chemistry and received PhD in Chemical Science from the University of Bologna. His research interests encompass chemistry, materials science and fabrication, with a focus on nanomaterials and their interactions with biological systems as well as functional organic/inorganic and hybrid materials for application in opto-electronics, sensing and data storage.

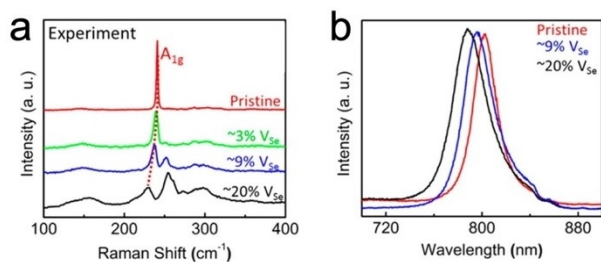


Figure 4. Evolution of optical properties vs. Se vacancy density in MoSe₂. (a) The Raman spectra. (b) PL spectra. The samples with higher vacancy density show a clear blue shift in their spectra with respect to the pristine samples which is proportional to defect density. Figure adapted from ref.^[11] with permission. Copyright 2016 American Chemical Society.

spectra on varying the percentage of Se atomic vacancies in MoSe₂ crystals. Photoluminescence and Raman spectroscopy are used to detect both the type and mean density of defects.

3.2. In-plane electrical conductivity

The presence of V_A defects strongly influences the electrical properties of semiconductors. For example, the most common defect in MoS₂, V_S, usually generates an n-type semiconductor.^[11–12] However, MoS₂ can be converted to p-type by substitutional doping of Mo atoms with electron-acceptor metal atoms, such as Nb,^[13] but also by regulating the density of V_S in the layer.^[6a] Importantly, in many cases, because of a non-uniform V_S distribution, different p- and n-type regions are present in the same sample, often compromising the predicted behaviour of the corresponding devices. On the other hand, when spatially controlled, an accurate electronic structure modulation allows the fabrication of 2D electronic devices such as 2D transistors and logic inverters.^[14]

V_A defects usually act as scattering centres which degrade the in-plane carrier mobility. The absolute value of charge mobility is very sensitive to the percentage of vacancies present. For example, in MoS₂, an increase in V_S from 0.1 to 3% can reduce the band mobility by several orders of magnitude.^[17] At the same time V_S defects create hopping centres activating new channels for charge transport^[14] which, became highly performant in optimized conditions, as recently demonstrated in a MoS₂ monolayer based field-effect transistor.^[4] It has also been calculated that in the case of spatially arranged V_S defects, the possible formation of percolation channels can enhance charge carrier mobilities at any given vacancy concentration, limiting the detrimental effects of electron scattering.^[6b] In-plane electrical conductivity of semiconductors is usually investigated using field-effect transistor configuration.^[4,15]

3.3. Resistive switching states

Besides the in-plane electrical conduction, V_A are responsible for resistive switching states in vertical junctions obtained by sandwiching the active material between metallic cross-bars or

electrical nano-contacts.^[16] This property has been exploited in memristors^[17] and atomistors (i.e. a memristor based on an atomically thin nanomaterial such as MoS₂ monolayers).^[18] In these devices the resistive switching is caused by the replacement of a V_S with a metal atom during the application of an appropriate pulsed bias and, remarkably, the filling of a V_A with consequent change in resistance can be non-volatile, but reversible.^[17a] The process is very efficient, but it is very sensitive to the V_S density and distribution, and this characteristic causes variations in the resistive states in different devices.

3.4. Tuning of thermal conductivity

The presence of V_A defects induces the formation of localized phonon states which strongly reduce thermal conductivity in defective materials.^[19] This effect is particularly relevant in 2D compounds and thin films consisting of only a few monolayers. Although the scattering strength of each phonon mode remains similar to that of the defect-free structure, localized phonon states reduce the phonon relaxation time²⁴ and significantly enhance the Umklapp scattering.^[19–20] As a consequence the thermal conductivity of the defective material is strongly reduced by the presence of V_A defects. For example, in MoS₂ single layers a 0.5% concentration of Mo vacancies can reduce the thermal conductivity by 60%.^[21]

3.5. Thermoelectricity

Acting upon both electrical and thermal conductivity to different extents, atomic vacancies strongly influence the performance of thermoelectric materials which can transform differences in temperature into changes in voltage.^[22] The efficiency of thermoelectric materials can be expressed by the figure of merit $ZT = \sigma S^2 T / (\kappa_e + \kappa_L)$, where S is the Seebeck coefficient, σ the electrical conductivity, T the absolute temperature and κ_e and κ_L are the electronic and lattice thermal conductivity, respectively. ZT maximization requires a large S , a high σ , and a low κ . However, these parameters are inter-dependent, thus ZT maximization is always challenging. Among the proposed approaches to improve ZT , V_A engineering has been considered by several theoretical articles as one of the most promising approaches,^[23] predicting a possible value of ZT higher than 6 even for defective MoS₂ monolayers. However, to date, experimental work has only reached a ZT of one order of magnitude lower than the predicted value. This discrepancy is attributed to the fact that the introduced dopants deteriorate the charge carrier mobility much more than expected, thus hindering the magnitude of ZT .

3.6. Catalysis

The presence of V_A defects can also produce materials for electrocatalysis.^[24] For example, defective transition metal dichalcogenides (TMDs) can be efficient and durable non-

precious metal electrocatalysts for a variety of important electrochemical reactions such as hydrogen or oxygen evolution through water splitting, the oxygen reduction reaction for polymer electrolyte fuel cells,^[25] or CO electroreduction.^[26] Chalcogenide vacancies generate localized electronic states in the lattice which act as sites for catalysis.^[27]

Besides the generation of catalytic sites, V_A defects also decrease the energy of hydrogen adsorption with a clear benefit for catalytic activity producing an excellent per-site turnover frequency for hydrogen evolution reactions (HERs).^[25,28] Figure 5 shows an example in which electrochemically fabricated V_S defects in MoS_2 enhance of one order of magnitude the HER catalytic activity with respect to pristine MoS_2 .^[25]

In general, electrocatalytic activity is proportional to the density of active sites and thus to V_A density, but V_A defects significantly reduce the electrical conductivity which has a detrimental effect on the kinetics and thus on the turnover rate of the electrochemical reactions.^[28]

3.7. Ion storage

Low-dimensional TMDs possess great potential as materials for Li and Na storage owing to their unique layered structures which can efficiently facilitate ion intercalation/deintercalation.^[29] The midgap states created by atomic vacancies (both V_{Metal} and $V_{\text{Non-metal}}$) act as active sites for substantial alkali-metal adsorption improving the specific capacity of the material. In addition, the rearrangement of atoms in the region of the vacancies not only promotes the adsorption positions of both Li and Na atoms at the defective site but also at sites around the atom vacancies. This effect, studied in MoS_2 , is caused by the local rearrangement of the lattice from a 2H configuration to a trigonal 1T configuration around the defects which further improves the storage capacity.^[29a,30] One major problem for ion storage is the reduction in electrical conductivity created by the vacancies and limits to the density of active sites which can be introduced in the materials without compromise its mechanical stability.

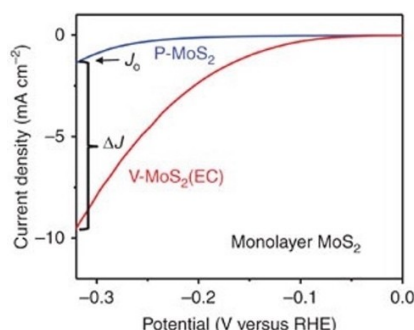


Figure 5. Linear sweep voltammetry of MoS_2 before (P- MoS_2) and after (V- MoS_2) sulphur vacancy formation. The current density increment is defined as $\Delta J/J_0$, where J_0 is the current density at -0.32 V versus RHE before desulfurization. Figure adapted from ref. 25 with permission. Copyright © 2017, The Authors.

3.8. Electrochemical supercapacitors

Defective TMDs have also been tested as electrochemical supercapacitors. Compared to pristine materials, defective materials proved to be more suitable electrode materials for electrochemical capacitors as the defects contribute to extra capacitance by introducing additional faradaic pseudo-capacitance or more exposed electrochemically active sites. In addition, in layered materials defects increase the surface area by increasing the interlayer distance.^[29b,31] As in the case of ion storage for batteries, major problems are related to the reduction of electrical conductivity due to the vacancies and limits to the number of active sites which can be introduced without compromising material stability.

3.9. Magnetism

Defect-induced magnetism is attracting interest for the production of ferromagnetic (FM) order in materials with only s and p electronic bands (most current FM order comes from d and f orbitals).^[32] Defect-induced magnetism is based on exchange interaction, which is a quantum mechanical mechanism between electron spins from nearest neighbours in the atomic lattice which determine the probability of alignment (or anti-alignment). The exchange interaction, whose strength is usually given by the exchange constant J , is basically a Coulomb interaction including the Pauli principle, thus it is very sensitive to spatial defect distribution. In 2D systems, the exchange interaction is extremely powerful and has stimulated a renaissance in the field of atomically thin magnets.^[33] Very few papers have investigated defective MoS_2 , in which FM is caused by the electronic states introduced by V_S in a 2H- MoS_2 ultrathin nanosheet host, which prompts the transformation of the surrounding 2H- MoS_2 local lattice into a trigonal (1T- MoS_2) phase.^[32] Calculations suggest that vacancy-doped MoS_2 monolayers can exhibit a high Curie temperature not too far from room temperature. However, although experiments confirm qualitatively theoretical predictions, the overall saturated magnetization measured is too low for use in practical applications.⁹

4. Defect formation and engineering

Customizing atomic vacancy defects to modulate the properties of defective materials can be achieved by controlling the synthesis parameters to obtain stoichiometry deviations during crystal growth or applying post-growth treatment to selectively create atomic defects.

4.1. Synthetic Methods

4.1.1. Chemical vapour transport

Chemical vapour transport (CVT) is the most common method used to grow crystals and films.^[1b,34] CVT involves the transport

of vaporized precursors in a sealed ampoule with a high temperature gradient (c.a. 1000 C°) along its length. CVT synthesis usually requires several days to obtain high-quality crystals which have to be exfoliated to be reduced to low-dimensional systems. The density and the nature of defects (atomic vacancies or substitutional atoms)^[35] is tuned by adjusting the initial loading of precursors and the experimental parameters (Temperature, flux, etc...). CVT allows a uniform statistical distribution of the point defects, but also generates a large number of edges, whose density can be inhomogeneous in the sample.^[36]

4.1.2. Chemical vapour deposition

Chemical vapour deposition (CVD) occurs by the chemical reaction of transition metals and non-metal gaseous precursors. It is used to produce and engineer both atomic vacancies and substitutional atoms. CVD synthesis occurs on a several-hours timescale and at lower temperatures compared to CVT.^[34] CVD provides a statistical distribution of defects. Typical problems consist of in-plane defect density gradients, or phase segregation. The quality of the defective crystal produced is very sensitive to experimental conditions and to the quality of the substrates (flatness, lattice constants, thermal stability and cleanliness) as they affect the orientation, size and shape of crystalline domains.

A large variety of defects can be generated and engineered in CVD-grown materials: i) the tuning of precursor composition determines the type of defects produced (vacancies and atom replacement); ii) by adjusting the flow of precursor vapour and temperature, it is possible to control the orientation of domains and the overall density of vacancies; iii) by varying the pressure and temperature, one can control the morphology of the sample (homogeneous thin films versus separated islands).

4.2. Post-growth treatments

Besides the defect generation during material-syntheses, several post-synthesis treatments have been developed for defect engineering. Post-growth treatment provides a greater degree of freedom for atomic-defect engineering and, in some cases, the spatial control of defective regions of the sample.^[44] Importantly, to obtain substitutional doping, the vacancies can be recovered by depositing different non-metallic atoms on the defective sample, as described below. There is a significant number of publications on various methods for post-growth treatments for defect generation and engineering, but here we discuss only the most common.

4.2.1. Thermal annealing

Thermal annealing is the simplest method of creating chalcogen atomic defects. Defect density can be regulated by acting upon the annealing temperature^[37] and on the environment.^[4]

When performed in an appropriate environment it can be directly used for atom replacement.^[38] There are some spatially controlled techniques which exploit thermal effects by locally heating a sample. For example, laser irradiation^[39] allows a spatial control on the micrometric scale and scanning thermochemical microscopy even at sub-micrometric levels.^[38] The ability to produce micropatterning using these techniques is a great advantage over thermal annealing, as it allow a spatial control of material functionalities, however upon the heating the atomic vacancies are mobile, migrating and agglomerating into vacancy lines or more complex defect aggregates.

4.2.2. Plasma treatment

Plasma treatment is an emerging strategy which can be conveniently exploited for engineering defects in materials. For example, the electrical properties of single-layer MoS₂ can be tuned from the semiconducting to the insulating regime through controlled exposure to oxygen plasma as the energetic oxygen molecules lead to the formation of insulating MoO₃-rich defect regions.^[40] On the other hand, treatment of TMD monolayers, such as WS₂, MoS₂ and WSe₂, with argon plasma creates atomic-scale defects with modification of their optical and electrical properties^[10] and in some cases a phase transition.^[41] Similarly, the introduction of selenium (Se) vacancies, following plasma treatment, leads to the phase conversion of semiconducting PdSe₂ to the metallic Pd₁₇Se₁₅ phase.^[42] The plasma experimental conditions allow a partial control of the defect density.

4.2.3. Electrochemical Methods

Electrochemical desorption has been demonstrated to be an efficient process for creating atomic vacancies in many conductive materials. For example, in MoS₂ the process occurs via proton and electron transfer to the sulphur atoms in the basal plane, with desorption of H₂S(g), leaving behind an S-vacancy.^[25] On changing the applied potential, the extent of desulfurization and the resulting activity can be varied. The method is very simple because it can be performed in a conventional electrochemical cell, by simply applying an appropriate ramp of potential at the electrode. The process allowed the fabrication of up to ca. 25% V₃ defects in the basal plane of MoS₂. Above this percentage the conductivity of MoS₂ is compromised and desorption became difficult. Moreover, the S-vacancy density was not spatially uniform across the surface, due to the clustering of S-vacancies. The electrochemical process for sulphur desorption has been used in various systems such as II-VI semiconductors,^[43] but is particularly efficient in the case of adsorbed layers.^[44] In addition, when combined with electrochemical lithographic techniques,^[45] such as the parallel local oxidation^[46] or reduction,^[47] electrochemical methods allow a spatial control with a resolution of a few tens of nanometres.

4.2.4. Electron-beam treatment

Electron-beam treatment is a serial method in which electron irradiation can be used to create precise nano-patterns of atomic defects in many materials. For example, e-beam irradiation at a few tens of keV were used to produce V_S and V_{2S} in MoS_2 layers.^[48] Defect formation in 2D can originate from various mechanisms which contribute synergistically to defect formation: mechanisms include ionization, beam-induced chemical etching, and ballistic displacement.^[48a] Careful regulation of experimental conditions allows the selective ejection of chalcogen atoms or, with greater irradiation, also of metal atoms. Figure 6 shows an example of V_S and V_{2S} fabricated on MoS_2 layers. When using state-of-the-art electron microscopes, e-beam treatment allows nanometric control of defect position. However, e-beam treatment can heat the sample locally which can create nano-holes, line defects or cracks in samples. Although this effect can compromise the spatial resolution of e-beam effects on the sample, it can be limited using an encapsulation procedure.^[48b]

4.2.5. Scanning Probe Microscopy

Besides the method previously described for the generation of V_A , most atomic scale engineering studies on surfaces have been performed via Scanning Probe Microscopy (SPM) in which atoms are handled individually in the fabrication of atomic vacancies^[49] or through the arrangement of surface atoms.^[50] All these experiments were performed in ultra-high vacuum and, apart from one case,^[50b] under cryogenic conditions, producing atomic patterns stable under the same experimental conditions used in the manufacturing process. In all cases the atoms are manipulated one by one, patterning areas of only a few hundred nanometres wide. SPM allows a real deterministic

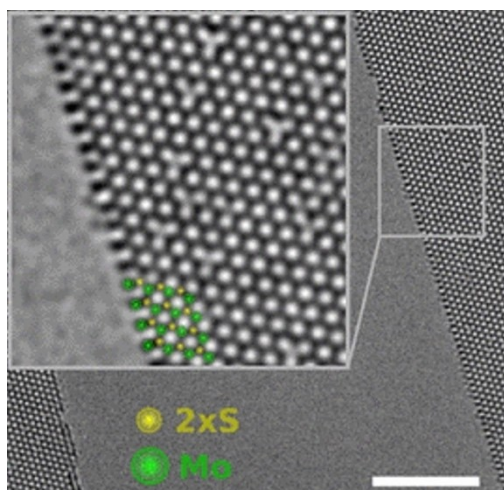


Figure 6. HR-TEM images MoS_2 layer. Atoms are dark and white spots which correspond to the holes in the hexagonal structure in which an increasing number of S vacancies is observed after e-beam irradiation. Both single vacancies and double vacancies can be found. Figure adapted from ref.[48a] with permission. Copyright © 2012, American Physical Society.

arrangement of V_A defects. Despite their absolute control in atom manipulation, SPM techniques have been hindered by the difficulties of experiments which can only be performed using sophisticated instrumentation and are limited by their intrinsic low throughput and the instability of the patterns produced, often stable only under the same experimental conditions used for their fabrication (i.e., ultra-high vacuum and cryogenic conditions).

4.2.6. Wet chemical methods

To date, despite their simplicity, wet chemical etching is not usually used for single-atom vacancy formation because of the practical difficulty in controlling the defect density and their distribution. As defects tend to aggregate during the processing, it isn't easy to obtain single-atom vacancies and uniform distributions. Only recently, Gao et al.^[14] demonstrated in MoS_2 that accurate control of etching agent concentration allows efficient management of defect density. Using a H_2O_2 aqueous solution, numerous single atom V_S were produced by the sulphur oxidation process, preserving the lattice stability. Although a systematic analysis of V_S density versus H_2O_2 concentration and treatment time was not directly reported, the evidence that the charge mobility of MoS_2 monolayer decreases with concentration and process duration of the treatment indirectly confirms the control of V_S density acting on these parameters.

4.2.7. Molecular-assisted vacancy formation

In a very recent work, we have demonstrated a new method for the electrochemical generation of single atomic vacancies at specific positions.^[51] The method consists of the electrochemical desorption of a non-metal atom assisted by a coordination compound molecule (CC). The CC works as a "molecular drone": it lands on a substrate (deposited or self-assembled on the surface), bonds to a specific atom on the surface forming a surface complex in which the surface atom bonded with the metal of the CC acting as its ligand, then upon the application of an electrochemical potential, much lower than the potential normally used for defect formation but capable of desorbing the CC with the surface atom, which then leaves the surface along with the extracted atom, thus creating an atomic vacancy in a specific position on the surface. Figure 7 shows the scheme of the process and the typical vacancies fabricated by molecular-assisted vacancy formation observed in-situ by STM. The feasibility of the process has been demonstrated under electrochemical control and with stability of the fabricated pattern at room temperature, under ambient conditions.

5. Atomic Vacancy Filling

As described above, atomic vacancies can be fabricated by various methods to obtain a wide variety of functional proper-

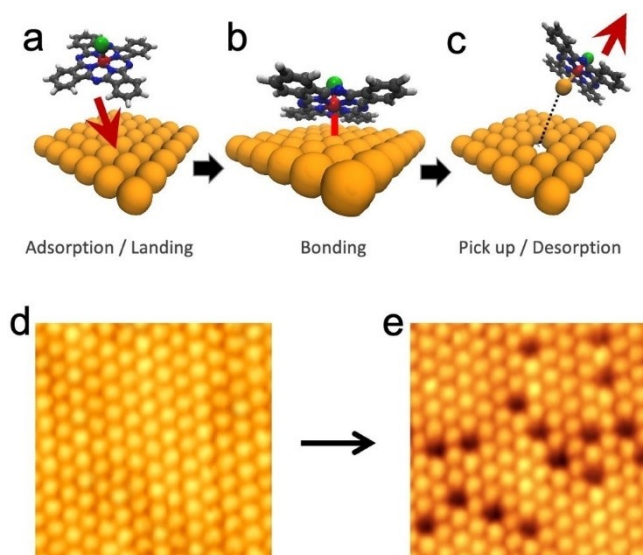


Figure 7. Concept of molecular-assisted vacancy formation. (a) A molecule of a Fe(III) phthalocyanine chloride is adsorbed on to the surface (an iodine-modified Ag surface), (b) it bonds to an atom of the surface forming a surface complex, and (c) it then leaves the surface along with the extracted atom. d–e) The process results in the creation of an atomic vacancy at the point where it had landed. In-situ STM images of the pristine I-modified Ag surface before (d) and after (e) the process. Bars are 2 nm. Figure adapted with permission from ref.51. Copyright 2021 Wiley.

ties. However, in some cases, atomic vacancies are unwanted as they can be detrimental for some desired properties of the materials. Thus, in parallel with the studies for their fabrication, strategies to fill atomic vacancies have been developed.^[11,52] Vacancy filling methods exploit the higher thermodynamic stability of defect-free materials compared to the defective ones. For example, in a recent work, Mahjouri-Samani et al. demonstrated that in Se-defective MoSe_{2-x} exposition of the sample to laser evaporated Se atoms leads to seleniation, filling the Se-vacant sites, thus recovering the properties of the pristine crystals.^[11] Recently, Zhao, X. et al. demonstrated that in the case of defective MoS_2 (both in the case of V_S and oxygen-substituted sulphur atoms) thermal annealing in H_2S remove almost quantitatively the V_S .^[52a] Vacancy filling has also been performed in solution. Recently, X. Zhang et al. established a powerful wet method for V_S filling in monolayer MoS_2 .^[52b] The authors showed that treatment in poly(4-styrenesulfonate) solution led to spontaneous V_S filling by the sulphur adatom on the MoS_2 surface. These techniques for the filling of atomic vacancies are very simple and efficient and can be used to introduce heteroatoms in vacancy-rich materials. Remarkably, using a thiol in substitution of dichalcogenides species, the process allows filling the atomic vacancy by the thiol itself, obtaining in a single step the surface functionalization.^[53]

6. Conclusions and Outlook

In this minireview we have considered the principal functionalities generated by the atomic vacancies of defective materials

for a variety of technological applications. We have summarized various pathways for fabricating atomic vacancies both during materials growth/synthesis and by post-growth treatments. The present methods are relatively simple and usually do not require advanced instrumentation. In addition, some post-growth treatments allow spatial control at the micrometric and sub-micrometric scales of the defective areas within the same sample. This extraordinary opportunity significantly expands opportunities for defective materials beyond conventional applications allowing, for example, the fabrication of devices fully fabricated within a single substrate modified locally.^[54]

Major problems include the limited number of defects which can be introduced in a material without altering their structure or compromising their mechanical stability and electrical conductivity. These are often the major drawbacks caused by the introduction of a high density of atomic vacancies. There are many open challenges of atomic vacancy engineering and more in general for defect engineering to be addressed: i) It is propaedeutic to defect engineering to be capable of fabricating defect-free materials in order to exercise real control of successive steps. To date, this is possible only for a limited number of materials, often using complex and expensive procedures; ii) Maximizing the density of defects without compromising the integrity of the material, thus moving toward customized defect distribution for specific devices; iii) Developing efficient deterministic control at sub-nanometric scale of the position of vacancies (defects) over large areas.

Once these problems have been addressed, we expect that defective materials can be a novel class of highly efficient materials and with programmed functionalities free of critical elements. In this context, theoretical calculations, including deep-learning and machine-learning configurations, are, and will be more and more in the future, a crucial tool in interpreting the properties generated by the defects, predicting their roles in material properties and stability and in optimizing their spatial distribution for specific applications. To date, the only technique which can obtain a real deterministic control of atomic vacancies on the atomic scale are SPL (Scanning Probe Lithography)-based techniques which, in some cases, have demonstrated the extraordinary potential of a real deterministic control of defect positioning. Unfortunately, SPL-based techniques are limited by low throughput in terms of time and very small areas. In the near future, we expect the development of novel deterministic processes for defect (vacancy) formation based on parallel approaches.

In conclusion, defect engineering and in particular atomic-vacancy engineering, is only at the beginning of their life, and thus there is an enormous amount of work to be done in order to reach an appreciable understanding of the techniques involved and a greater spatial control over much larger areas. Once reached, we expect an enormous impact of the development of defect-containing materials in science and technology, opening new opportunities in materials science.

Acknowledgements

We thank Derek Jones for his help and critical review. We are grateful for the financial support provided by the Italian Minister of Instruction, University and Research, National Project PRIN "Novel Multilayered and Micro-Machined Electrodes, Nano-Architectures for Electrocatalytic Applications". Prot. 2017YH9MRK. Open Access Funding provided by Consiglio Nazionale delle Ricerche within the CRUI-CARE Agreement.

Conflict of Interest

The authors declare no conflict of interest.

Keywords: atomic defects · doping · surface chemistry · thin films · transition metal dichalcogenides

- [1] a) Q. Liang, Q. Zhang, X. Zhao, M. Liu, A. T. S. Wee, *ACS Nano* **2021**, *15*, 2165–2181; b) Z. Lin, B. R. Carvalho, E. Kahn, R. Lv, R. Rao, H. Terrones, M. A. Pimenta, M. Terrones, *2D Mater.* **2016**, *3*, 022002; c) J. Jiang, T. Xu, J. Lu, L. Sun, Z. Ni, *Research* **2019**, *2019*, 4641739; d) Z. Lin, A. McCreary, N. Briggs, S. Subramanian, K. H. Zhang, Y. F. Sun, X. F. Li, N. J. Borys, H. T. Yuan, S. K. Fullerton-Shirey, A. Chernikov, H. Zhao, S. McDonnell, A. M. Lindenberg, K. Xiao, B. J. LeRoy, M. Drndic, J. C. M. Hwang, J. Park, M. Chhowalla, R. E. Schaak, A. Javey, M. C. Hersam, J. Robinson, M. Terrones, *2D Mater.* **2016**, *3*, 042001.
- [2] X. Zhang, L. Gao, H. Yu, Q. Liao, Z. Kang, Z. Zhang, Y. Zhang, *Acc. Mater. Res.* **2021**, *2*, 655–668.
- [3] D. Rhodes, S. H. Chae, R. Ribeiro-Palau, J. Hone, *Nat. Mater.* **2019**, *18*, 541–549.
- [4] X. K. Zhang, Q. L. Liao, Z. Kang, B. S. Liu, X. Z. Liu, Y. Ou, J. K. Xiao, J. L. Du, Y. H. Liu, L. Gao, L. Gu, M. Y. Hong, H. H. Yu, Z. Zhang, X. F. Duan, Y. Zhang, *Adv. Mater.* **2021**, *33*, 2007051.
- [5] W. Zhou, X. Zou, S. Najmaei, Z. Liu, Y. Shi, J. Kong, J. Lou, P. M. Ajayan, B. I. Yakobson, J.-C. Idrobo, *Nano Lett.* **2013**, *13*, 2615–2622.
- [6] a) J. Yang, F. Bussolotti, H. Kawai, K. E. J. Goh, *Phys. Status Solidi RRL* **2020**, *14*, 2000248; b) S. M. Gali, A. Pershin, A. Lherbier, J. C. Charlier, D. Beljonne, *J. Phys. Chem. C* **2020**, *124*, 15076–15084.
- [7] H.-P. Komsa, A. V. Krasheninnikov, *Phys. Rev. B* **2015**, *91*, 125304.
- [8] L. M. Malard, T. V. Alencar, A. P. M. Barboza, K. F. Mak, A. M. de Paula, *Phys. Rev. B* **2013**, *87*, 201401.
- [9] K. F. Mak, K. He, C. Lee, G. H. Lee, J. Hone, T. F. Heinz, J. Shan, *Nat. Mater.* **2013**, *12*, 207–211.
- [10] a) P. K. Chow, R. B. Jacobs-Gedrim, J. Gao, T.-M. Lu, B. Yu, H. Terrones, N. Koratkar, *ACS Nano* **2015**, *9*, 1520–1527; b) Z. T. Wu, W. W. Zhao, J. Jiang, T. Zheng, Y. M. You, J. P. Lu, Z. H. Ni, *J. Phys. Chem. C* **2017**, *121*, 12294–12299.
- [11] M. Mahjouri-Samani, L. Liang, A. Oyedele, Y.-S. Kim, M. Tian, N. Cross, K. Wang, M.-W. Lin, A. Boulesbaa, C. M. Rouleau, A. A. Puzos, K. Xiao, M. Yoon, G. Eres, G. Duscher, B. G. Sumpter, D. B. Geohegan, *Nano Lett.* **2016**, *16*, 5213–5220.
- [12] H. Qiu, T. Xu, Z. Wang, W. Ren, H. Nan, Z. Ni, Q. Chen, S. Yuan, F. Miao, F. Song, G. Long, Y. Shi, L. Sun, J. Wang, X. Wang, *Nat. Commun.* **2013**, *4*, 2642.
- [13] M. Li, J. Yao, X. Wu, S. Zhang, B. Xing, X. Niu, X. Yan, Y. Yu, Y. Liu, Y. Wang, *ACS Appl. Mater. Interfaces* **2020**, *12*, 6276–6282.
- [14] L. Gao, Q. Liao, X. Zhang, X. Liu, L. Gu, B. Liu, J. Du, Y. Ou, J. Xiao, Z. Kang, Z. Zhang, Y. Zhang, *Adv. Mater.* **2020**, *32*, 1906646.
- [15] L. Wang, L. Chen, S. L. Wong, X. Huang, W. Liao, C. Zhu, Y.-F. Lim, D. Li, X. Liu, D. Chi, K.-W. Ang, *Adv. Electr. Mater.* **2019**, *5*, 1900393.
- [16] M. Cavallini, Z. Hemmatian, A. Riminucci, M. Prezioso, V. Morandi, M. Murgia, *Adv. Mater.* **2012**, *24*, 1197–1201.
- [17] a) S. M. Hus, R. J. Ge, P. A. Chen, L. B. Liang, G. E. Donnelly, W. Ko, F. M. Huang, M. H. Chiang, A. P. Li, D. Akinwande, *Nat. Nanotechnol.* **2021**, *16*, 2165–2181; b) X. H. Wu, R. J. Ge, D. Akinwande, J. C. Lee, *Nanotechnol.ogy* **2020**, *31*, 465206.
- [18] R. Ge, X. Wu, M. Kim, J. Shi, S. Sonde, L. Tao, Y. Zhang, J. C. Lee, D. Akinwande, *Nano Lett.* **2018**, *18*, 434–441.
- [19] B. Peng, Z. Ning, H. Zhang, H. Shao, Y. Xu, G. Ni, H. Zhu, *J. Phys. Chem. C* **2016**, *120*, 29324–29331.
- [20] Y. Wu, Z. Chen, P. Nan, F. Xiong, S. Lin, X. Zhang, Y. Chen, L. Chen, B. Ge, Y. Pei, *Joule* **2019**, *3*, 1276–1288.
- [21] Z. Ding, Q.-X. Pei, J.-W. Jiang, Y.-W. Zhang, *J. Phys. Chem. C* **2015**, *119*, 16358–16365.
- [22] A. Majumdar, *Science* **2004**, *303*, 777–778.
- [23] a) M. Sharma, A. Kumar, P. K. Ahluwalia, *Phys. E: Low-dimens. Syst. Nanostruct.* **2019**, *107*, 117–123; b) C. Adessi, S. Pecoraro, S. Thébaud, G. Bouzerar, *Phys. Chem. Chem. Phys.* **2020**, *22*, 15048–15057.
- [24] Y. N. Guo, T. Park, J. W. Yi, J. Henzie, J. Kim, Z. L. Wang, B. Jiang, Y. Bando, Y. Sugahara, J. Tang, Y. Yamauchi, *Adv. Mater.* **2019**, *31*, 1807134.
- [25] C. Tsai, H. Li, S. Park, J. Park, H. S. Han, J. K. Nørskov, X. L. Zheng, F. Abild-Pedersen, *Nat. Commun.* **2017**, *8*, 15113.
- [26] D. X. Jiao, Y. Tian, Y. J. Liu, Q. H. Cai, J. X. Zhao, *Sustain. Energy Fuels* **2021**, *5*, 4932–4943.
- [27] a) X. Yan, L. Zhuang, Z. Zhu, X. Yao, *Nanoscale* **2021**, *13*, 3327–3345; b) C. Meng, X. Chen, Y. Gao, Q. Zhao, D. Kong, M. Lin, X. Chen, Y. Li, Y. Zhou, *Molecules* **2020**, *25*, 1136.
- [28] H. Li, C. Tsai, A. L. Koh, L. Cai, A. W. Contryman, A. H. Fragapane, J. Zhao, H. S. Han, H. C. Manoharan, F. Abild-Pedersen, J. K. Nørskov, X. Zheng, *Nat. Mater.* **2016**, *15*, 48–53.
- [29] a) G. Barik, S. Pal, *J. Phys. Chem. C* **2019**, *123*, 21852–21865; b) H. Liu, W. Lei, Z. Tong, X. Li, Z. Wu, Q. Jia, S. Zhang, H. Zhang, *Adv. Mater. Interfaces* **2020**, *7*, 2000494.
- [30] A. Meng, T. Huang, H. Li, H. Cheng, Y. Lin, J. Zhao, Z. Li, *J. Colloid Interface Sci.* **2021**, *589*, 147–156.
- [31] N. Joseph, P. M. Shafi, A. C. Bose, *Energy Fuels* **2020**, *34*, 6558–6597.
- [32] L. Cai, J. F. He, Q. H. Liu, T. Yao, L. Chen, W. S. Yan, F. C. Hu, Y. Jiang, Y. D. Zhao, T. D. Hu, Z. H. Sun, S. Q. Wei, *J. Am. Chem. Soc.* **2015**, *137*, 2622–2627.
- [33] a) D. L. Cortie, G. L. Causer, K. C. Rule, H. Fritzsche, W. Kreuzpaintner, F. Klose, *Adv. Funct. Mater.* **2020**, *30*, 1901414; b) P. Esquinazi, W. Hergert, D. Spemann, A. Setzer, A. Ernst, *IEEE Trans. Magn.* **2013**, *49*, 4668–4674.
- [34] Y. Shi, H. Li, L.-J. Li, *Chem. Soc. Rev.* **2015**, *44*, 2744–2756.
- [35] Q. Zeng, H. Wang, W. Fu, Y. Gong, W. Zhou, P. M. Ajayan, J. Lou, Z. Liu, *Small* **2015**, *11*, 1868–1884.
- [36] H. Li, G. Lu, Y. Wang, Z. Yin, C. Cong, Q. He, L. Wang, F. Ding, T. Yu, H. Zhang, *Small* **2013**, *9*, 1974–1981.
- [37] H. Zhu, Q. Wang, L. Cheng, R. Addou, J. Kim, M. J. Kim, R. M. Wallace, *ACS Nano* **2017**, *11*, 11005–11014.
- [38] X. Zheng, A. Calò, T. Cao, X. Liu, Z. Huang, P. M. Das, M. Drndic, E. Albisetti, F. Lavini, T.-D. Li, V. Narang, W. P. King, J. W. Harrold, M. Vittadello, C. Aruta, D. Shahrjerdi, E. Riedo, *Nat. Commun.* **2020**, *11*, 3463.
- [39] S. Cho, S. Kim, J. H. Kim, J. Zhao, J. Seok, D. H. Keum, J. Baik, D.-H. Choe, K. J. Chang, K. Suenaga, S. W. Kim, Y. H. Lee, H. Yang, *Science* **2015**, *349*, 625.
- [40] M. R. Islam, N. Kang, U. Bhanu, H. P. Paudel, M. Erementchouk, L. Tetard, M. N. Leuenberger, S. I. Khondaker, *Nanoscale* **2014**, *6*, 10033–10039.
- [41] J. Q. Zhu, Z. C. Wang, H. Yu, N. Li, J. Zhang, J. L. Meng, M. Z. Liao, J. Zhao, X. B. Lu, L. J. Du, R. Yang, D. Shi, Y. Jiang, G. Y. Zhang, *J. Am. Chem. Soc.* **2017**, *139*, 10216–10219.
- [42] M. S. Shawkat, J. Gil, S. S. Han, T.-J. Ko, M. Wang, D. Dev, J. Kwon, G.-H. Lee, K. H. Oh, H.-S. Chung, T. Roy, Y. Jung, Y. Jung, *ACS Appl. Mater. Interfaces* **2020**, *12*, 14341–14351.
- [43] M. Innocenti, S. Cattarin, M. Cavallini, F. Loglio, M. L. Foresti, *J. Electroanal. Chem.* **2002**, *532*, 219–225.
- [44] a) M. Cavallini, G. Aloisi, R. Guidelli, *Langmuir* **1999**, *15*, 2993–2995; b) G. D. Aloisi, M. Cavallini, M. Innocenti, M. L. Foresti, G. Pezzatini, R. Guidelli, *J. Phys. Chem. B* **1997**, *101*, 4774–4780.
- [45] F. C. Simeone, C. Albonetti, M. Cavallini, *J. Phys. Chem. C* **2009**, *113*, 18987–18994.
- [46] M. Cavallini, P. Mei, F. Biscarini, R. Garcia, *Appl. Phys. Lett.* **2003**, *83*, 5286–5288.
- [47] M. Cavallini, P. Graziosi, M. Calbucci, D. Gentili, R. Cecchini, M. Barbalinardo, I. Bergenti, A. Riminucci, V. Dediu, *Sci. Rep.* **2014**, *4*, 1–4.
- [48] a) H.-P. Komsa, J. Kotakoski, S. Kurasch, O. Lehtinen, U. Kaiser, A. V. Krasheninnikov, *Phys. Rev. Lett.* **2012**, *109*, 035503; b) R. Zan, Q. M. Ramasse, R. J. Ge, T. Georgiou, U. Bangert, K. S. Novoselov, *ACS Nano* **2013**, *7*, 10167–10174.

- [49] F. E. Kalff, M. P. Rebergen, E. Fahrenfort, J. Girovsky, R. Toskovic, J. L. Lado, J. Fernandez-Rossier, A. F. Otte, *Nat. Nanotechnol.* **2016**, *11*, 926–929.
- [50] a) M. Schunack, E. Laegsgaard, I. Stensgaard, I. Johannsen, F. Besenbacher, *Angew. Chem. Int. Ed.* **2001**, *40*, 2623–2626; *Angew. Chem.* **2001**, *113*, 2693–2696; b) Y. Sugimoto, P. Pou, O. Custance, P. Jelinek, M. Abe, R. Perez, S. Morita, *Science* **2008**, *322*, 413–417.
- [51] M. Baldoni, F. Mercuri, M. Cavallini, *Adv. Mater.* **2021**, *33*, 2007150.
- [52] a) X. Zhao, P. Song, C. Wang, A. C. Riis-Jensen, W. Fu, Y. Deng, D. Wan, L. Kang, S. Ning, J. Dan, T. Venkatesan, Z. Liu, W. Zhou, K. S. Thygesen, X. Luo, S. J. Pennycook, K. P. Loh, *Nature* **2020**, *581*, 171–177; b) X. Zhang, Q. Liao, S. Liu, Z. Kang, Z. Zhang, J. Du, F. Li, S. Zhang, J. Xiao, B. Liu, Y. Ou, X. Liu, L. Gu, Y. Zhang, *Nat. Commun.* **2017**, *8*, 15881.
- [53] D. M. Sim, M. Kim, S. Yim, M.-J. Choi, J. Choi, S. Yoo, Y. S. Jung, *ACS Nano* **2015**, *9*, 12115–12123.
- [54] M. Melucci, M. Zambianchi, L. Favaretto, V. Palermo, E. Treossi, M. Montalti, S. Bonacchi, M. Cavallini, *Chem. Commun.* **2011**, *47*, 1689–1691.

Manuscript received: December 29, 2021
Revised manuscript received: March 3, 2022
Accepted manuscript online: March 11, 2022